Research Article

gazi JOURNAL OF ENGINEERING SCIENCES

Gazi AKADEMİK YAYINCILIK

GAZİ
JOURNAL OF ENGINEERING SCIENCES

Heading Estimation for Agricultural Vehicles with Multi-Antenna RTK/GNSS, Tactical-Grade and Low-Cost IMUs

Hasan Dilmac[a], Veli Ilci[*b], Emirhan Kaya[c]

Submitted: 28.01.2025 Revised: 25.03.2025 Accepted: 13.04.2025 doi:10.30855/gmbd.070525N10

Keywords: Autonomous vehicles, heading determination, GNSS, IMU

[a] Ondokuz Mayis University, Faculty of Engineering, Dept. of Geomatics Engineering 55139 - Samsun, Türkiye
Orcid: 0000-0001-6877-8730
e mail: hasan.dilmac@omu.edu.tr

[b,*] Ondokuz Mayis University, Faculty of Engineering, Dept. of Geomatics Engineering 55139 - Samsun, Türkiye
Orcid: 0000-0002-9485-874X

[c] Ondokuz Mayis University, Faculty of Engineering, Dept. of Geomatics Engineering 55139 - Samsun, Türkiye
Orcid: 0009-0007-2633-3419

*Corresponding author: veli.ilci@omu.edu.tr

ABSTRACT

Nowadays, Autonomous Vehicles (AVs) are employed for various tasks, including spraying, harvesting, and planting. For AVs to navigate autonomously, accurate heading knowledge of the vehicle is essential. Sensors such as the Global Navigation Satellite System (GNSS) and Inertial Measurement Unit (IMU) are used on AVs to produce heading information. Dual-frequency and Real-Time Kinematic (RTK) capable systems with multiple antennas are used to increase the heading accuracy of GNSS. For IMUs, heading accuracy is directly related to the quality of the sensors, so high accuracy is achieved with expensive IMUs. However, with the development of micro-electro-mechanical system (MEMS) technology, studies are also being carried out on low-cost IMU solutions. This study tested the heading performances of three different sensors: a low-cost RTK/GNSS with multiple antennas, a tactical-grade IMU, and a low-cost MEMS IMU. An Unmanned Ground Agricultural Vehicle (UGAV) designed for spraying was driven on a line, and the sensors' data mounted on the UGAV were collected. Heading accuracy was also examined according to the distance between the RTK/GNSS system antennas. As a result of the analysis, the average errors of RTK/GNSS, tactical-grade IMU, and low-cost IMU are 0.58, 0.60, and 4.24 degrees, respectively.

Tarım Araçları için Çok-Antenli RTK/GNSS, Taktiksel-Sınıf ve Düşük-Bütçeli IMU ile Yön Tahmini

ÖZ

Günümüzde Otonom Araçlar (AVs), ilaçlama, hasat ve ekim gibi çok çeşitli görevlerde kullanılmaktadır. OA'ların otonom bir şekilde hareket edebilmesi için aracın doğru yön bilgisi esastır. OA'larda yön bilgisi üretmek için Küresel Navigasyon Uydu Sistemi (GNSS) ve Ataletsel Ölçü Birimi (IMU) gibi sensörler kullanılır. Gerçek Zamanlı Kinematik (RTK) çözümü sağlayabilen çift frekanslı çoklu antenlere sahip sistemler, GNSS'in yön belirleme doğruluğunu artırmak için kullanılabilmektedir. IMU'lar için yön doğruluğu sensörlerin kalitesiyle ilgilidir, bu nedenle pahalı IMU'larla yüksek doğruluk elde edilir. Ancak Mikro-Elektro Mekanik Sistem (MEMS) teknolojisinin gelişmesiyle birlikte düşük maliyetli IMU çözümleri üzerinde de çalışmalar yürütülmektedir. Bu çalışmada, çoklu antene sahip düşük maliyetli bir RTK/GNSS, taktiksel sınıf bir IMU ve düşük maliyetli bir MEMS IMU olmak üzere üç farklı sensörün yön belirleme performansları test edilmiştir. İlaç püskürtme için tasarlanmış İnsansız Kara Tarım Aracıyla (UGAV) bir hat üzerinde sürüş gerçekleştirilmiş ve üzerine monte edilmiş sensörlerle veriler toplanmıştır. Ayrıca, RTK/GNSS sisteminin antenleri arasındaki mesafeye göre elde ettiği yön doğruluğu da incelenmiştir. Analiz sonucunda, RTK/GNSS, taktiksel sınıf IMU ve düşük maliyetli IMU'nun ortalama hataları sırasıyla 0,58, 0,60 ve 4,24 derece bulunmuştur.

Anahtar Kelimeler: Otonom araçlar, yön tahmini, GNSS, IMU

To cite this article: H. Dilmac, V. Ilci and E. Kaya, "Heading Estimation for Agricultural Vehicles with Multi-Antenna RTK/GNSS, Tactical-Grade and Low-Cost IMUs", *Gazi Journal of Engineering Sciences,* vol.11, no.1, pp. 153-166, 2025. doi:10.30855/gmbd.070525N10

1. Introduction

Precision agriculture is becoming an important research area due to population growth, climate change, and global warming. Furthermore, by 2050, 70% of the world's population is expected to reside in cities, creating a shortage of workers in rural areas [1]. Because of this, there is an increasing need for automation, and new techniques and tools are required to monitor and examine plants and crops in addition to increasing farming output [2]. Future agricultural concepts include more sophisticated farms with sensors, machinery, and robots that are more productive and environmentally sustainable. Autonomous Vehicles (AVs) and robotics have the potential to be crucial in achieving the demands of agricultural products in this regard [3]. Many tasks, including weeding [4], spraying [5], planting and harvesting [6-8], monitoring the environment [9], and supplying water and fertilisers [10], are being performed by autonomous vehicles and robots in agriculture.

Self-localization is an essential component of AVs in fulfilling their mission in the field. Early navigation systems are primarily based on vision sensors and computer vision techniques [11]. Over the past decades, autonomous localisation of AVs has been addressed by different kinds of methods, including Global Navigation Satellite Systems (GNSS), Light Detection and Ranging (LiDAR), and Inertial Measurement Units (IMUs) [12]. GNSS-based localisation has been the most applied approach for AVs [13,14]. By implementing three different control strategies, Alonso-Garcia et al. [15] assessed the effectiveness of low-cost GNSS receivers in enabling the autonomous navigation of agricultural tractors. Han et al. [16] introduced a path planning and tracking system for an autonomous agricultural sprayer using a single-frequency GNSS Real-Time Kinematic (RTK), achieving a positional accuracy of 0.01 m.

Estimating the vehicle's heading is another crucial task in autonomous navigation [17]. Even though the price of GNSS devices has been dropping recently, most studies still use IMU sensors like 3-axis Fiber Optical Gyroscopes (FOG) for vehicle heading estimation [18]. Three-axis FOGs are typically paired with three-axis accelerometers and magnetometers to find and track vehicles' position and heading. However, since sensor drift causes them to accumulate motion estimation errors, their primary purpose in navigation is short-range [19]. Besides, FOG sensors are quite costly, making their usage in agricultural robots unfeasible [20]. This has led to the widespread use of commercially available, low-cost Micro-Electro-Mechanical System (MEMS) IMUs in low-grade inertial systems. However, this technology is still in its infancy, and its benefits come at the risk of poor accuracy [21]. Compared to its optical equivalents, low-cost MEMS exhibit much worse accuracy because of more significant biases, axis misalignment errors, scale factor, and increased temperature drift susceptibility [22]. Since MEMS IMUs have a limited capacity, they are generally combined with other sensors to improve heading accuracy [23,24]. A vehicle's position, velocity, and heading can be accurately determined via GNSS, which is suitable for autonomous driving operations. By utilising the vehicle's current position and heading, the GNSS-based autonomous driving approach computes the optimal steering angle and wheel speed based on predefined waypoints, enabling the vehicle to accurately follow a predetermined route [25]. GNSS can typically provide a position solution with an accuracy of a few meters. It is possible to attain sub-meter precision, but it will take extra processing and external data. For instance, the RTK method is used in GNSS to obtain cm-level accuracy [26]. RTK/GNSS is typically used to find a stationary rover's position. However, it can also be used to determine the exact location of a moving rover antenna on a vehicle. It is even possible to ascertain the platform's heading by installing many antennas on it [27]. Nadarajah et al. [28] examined the single-frequency GNSS attitude determination performance utilising a combination of GPS and Galileo measurements. Zhu et al. [29] combined MEMS IMU with dual-antenna GNSS to get attitude information in a GNSS-limited environment with high accuracy.

Today, the accuracy and precision required for the heading and location of AVs can be achieved with costly systems. However, this is one of the biggest obstacles to the commercialisation and widespread use of AVs. Therefore, some studies were undertaken to provide the required accuracy and sensitivity with low-cost sensors [30, 31]. This study analysed the heading estimation accuracies of a low-cost RTK/GNSS with triple antennas, tactical grade, and low-cost MEMS IMUs. For this purpose, a vehicle designed for agricultural spraying was driven along a straight line, and heading predictions were made with sensors. In addition, it was evaluated how the distance between the antennas of the RTK/GNSS affected the heading accuracy. This paper is organised as follows. Section II presents the vehicle system and sensor placement, heading estimation methods of sensors, analysis methods, and field experiment. Section III gives the heading estimation results for the sensors. Finally, the conclusions of this study are included in Section IV.

2. Material and Methods

2.1. The vehicle system and sensor placement

An Unmanned Ground Agricultural Vehicle (UGAV) designed for agricultural spraying was used to analyse the heading performances of the sensors. The design of the vehicle is shown in Figure 1a. However, to analyse the heading accuracy of RTK/GNSS according to the distances between the antennas, additional parts were mounted on UGAV, and the distance between the antennas was adjusted accordingly (Figure 1b). A total of 7 separate drives was made to determine the heading accuracy according to the varying distance between RTK/GNSS antennas. The position of the first antenna (ANT1) was fixed, and the second antenna (ANT2) was moved at intervals of 30 cm in a north-south direction, at most 210 cm and at least 30 cm away from the ANT1. In each drive, heading estimation was also obtained with tactical grade and low-cost IMUs for comparison purposes. Since the content of the study is related to the heading, the ANT3 was not used even though it was placed on the vehicle.

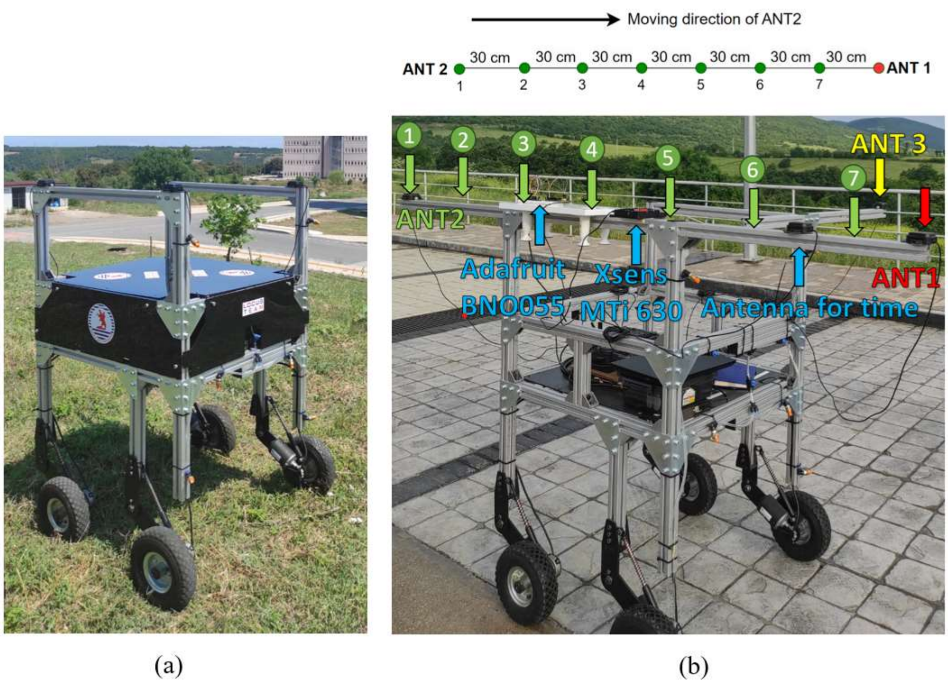

Figure 1. UGAV (a) standard design; (b) modified design for setting antenna distance.

2.2. Heading estimation based on RTK/GNSS

A simpleRTK2B SBC development board [32], a multi-frequency GNSS sensor, was utilised in the study. Three u-blox ZED-F9 modules and three GNSS antennas can be used simultaneously on this board (Figure 2). This development board is open code and programmable. This allows the development of algorithms for many different applications. This development card can receive RTK corrections for all three antennas, so the position of each antenna can be obtained with cm precision (Table 1). It is a low-cost RTK-GNSS sensor compared to its equivalents in the market.

Table 1. Sensor specifications

Specifications	SimpleRTK2B SBC	Xsens Mti 630	Adafruit BNO055
Price	• $1,033.85	• €1,009.00	• $34.95
Type	• Low-cost GNSS	• Tactical-Grade IMU	• Low-Cost IMU
Positional Accuracy	• <1-4 cm with corrections • <1.5m in standalone mode	-	-
Heading Accuracy	• Sub-degree	• ±1 degree	• ±2.5 degree
Update Rate	• Up to 20Hz	• Up to 400Hz	• Up to 100Hz
Advantages	• High positional accuracy (RTK cm-level precision) • Three-Dimensional (3D) position information beside the heading • Optimal in open-sky environment • Provide Coordinated Universal Time (UTC) time	• High heading accuracy • High frequency • Provide UTC	• Low-cost compared to the other sensors • Compact and easy to integrate • Suitable for basic orientation tracking
Disadvantages	• Requires GNSS signal for operation (limited indoor use)	• Requires calibration • Susceptible to magnetic interference affecting heading accuracy	• Requires calibration • Highly sensitive to magnetic interference • Lower heading accuracy compared to high-end IMUs

GNSS delivers two primary types of measurements: carrier phase and pseudorange. If the carrier phase ambiguity can be successfully resolved, the positioning based on the carrier phase yields a more precise range than those using pseudorange.

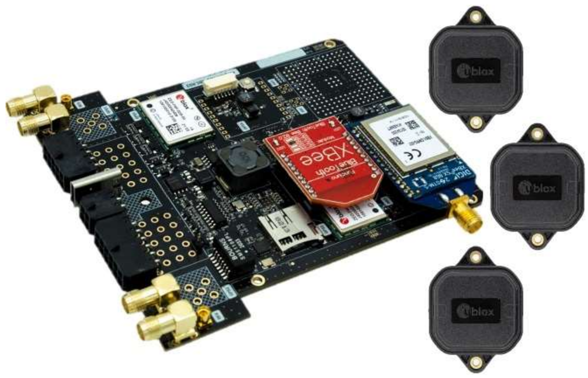

Figure 2. SimpleRTK2B SBC

Ambiguity resolution is one of the most challenging issues in GNSS and is a necessary first step for all RTK positioning-related applications [33]. In the RTK approach, which presents the ideas of a base and a rover, one or more rovers receive a continuous differential correction data stream (per the RTCM 3.3 protocol) from the base over a communication channel (Figure 3). In the standard RTK, the base stays in a static known position. However, this is not the case for mobile vehicles carrying both the base and the rover. For this, a moving base RTK approach is developed so that both base and rover receivers can move. With the moving base RTK approach, heading estimation of a moving vehicle can be obtained [27].

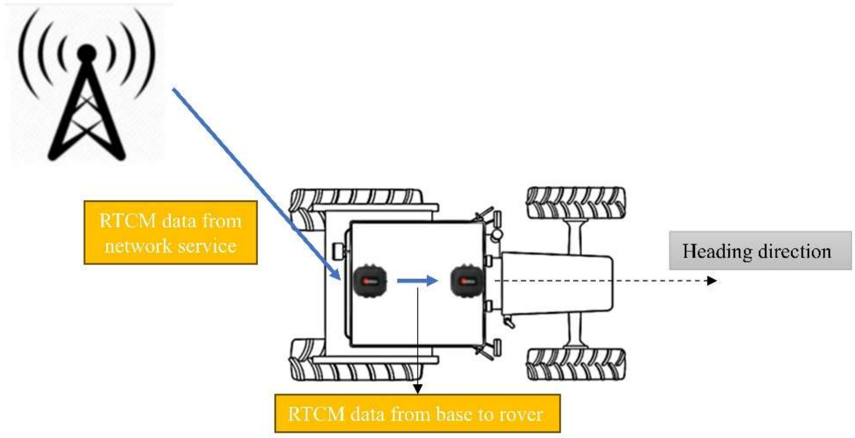

Figure 3. Moving base setup for heading estimation [34]

Several coordinate systems are utilised in heading determination using GNSS. The local level coordinate system is commonly employed as the reference for calculating the heading of a moving vehicle. This topocentric coordinate system is defined relative to a reference ellipsoid, such as GRS80. Another coordinate system is the vehicle platform coordinate system defined by the user. The heading direction coincides with the vehicle's direction of travel [35]. Then, the heading of the vehicle to the reference system can be estimated by using two GNSS antennas as below:

$$\Psi_G = \text{atan}\left(\frac{Y_{ANT2} - Y_{ANT1}}{X_{ANT2} - X_{ANT1}}\right) \quad (1)$$

Here, Ψ_G is grid heading. The SimpleRTK2B SBC development board provides GNGGA via the National Marine Electronics Association (NMEA) messages containing the geographic coordinates, time, and other information about the antennas. The grid coordinates of the points in the Transverse Mercator (TM) projection were generated for the heading estimation.

2.3. Heading estimation based on IMUs

In this study, a tactical-grade MEMS IMU (Xsens Mti 630), and a low-cost IMU (Adafruit BNO055) were used to estimate the vehicle's heading. Xsens Mti-630 includes a 3-axis gyroscope, 3-axis accelerometer, 3-axis magnetometer, control and fusion unit. With the control unit, timing and synchronisation of the sensors is ensured. At the same time, it provides motion data at high frequencies using calibration models and an Xsens-optimized strap-down algorithm. Thanks to the sensor fusion units inside, Xsens combines the information from all sensors and, as a result, provides location and true north-referenced heading data at frequencies up to 400 Hz [36]. Xsens Mti Manager software was used to communicate with the Xsens Mti 630 to get data files and set some parameters (coordinate system, time update, output preference, filter settings to get true north-referenced heading or true heading (Ψ_T)).

Adafruit BNO055 sensor also has a 3-axis gyroscope, 3-axis accelerometer, and 3-axis magnetometer sensors [37]. However, it is a low-cost MEMS sensor with a lower capacity than Xsens Mti 630. Some raw data such as linear acceleration (a_x, a_y, a_z in m s^{-2}), angular velocity (w_x, w_y, w_y in deg s^{-1}), magnetic field vector (m_x, m_y, m_z in Tesla m^{-2}), and calibration information can be received from the Adafruit BNO055 sensor.

Arduino Nano was used to receive and process the data of the Adafruit BNO055 sensor. Unlike other sensors (SimpleRTK2B SBC and Xsens MTi 630), BNO055 does not provide UTC. In the study, another sensor, SimpleRTK 2B, was used to allow the comparison of different sensor outputs based on UTC. Both sensors were connected via Arduino, and raw IMU data was obtained along with UTC (Figure 4).

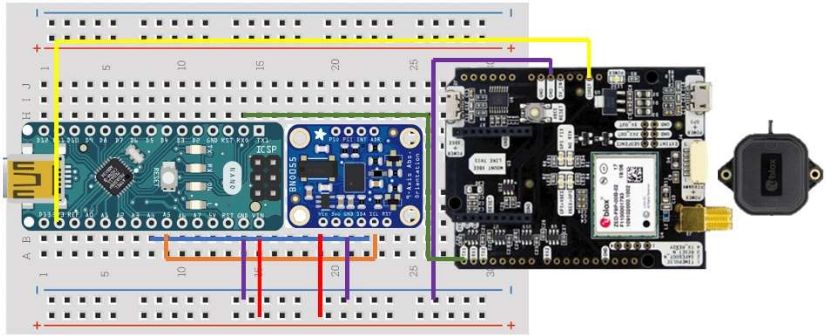

Figure 4. Arduino Nano, Adafruit, and SimpleRTK2B connection diagram

Just as a gravitational vector (g) is applied to objects towards the center of the earth, a magnetic vector is coming towards objects from the magnetic north. For a situation where pitch and roll angles also come into play, that is, where there is movement in 3D space rather than in a horizontal plane, heading calculation is made as follows [38]:

$$\Psi_M = \text{atan}\left(\frac{m_y * cos(\emptyset) + m_z * \sin(\emptyset)}{m_x * \cos(\theta) - m_y * \sin(\emptyset) * \sin(\theta) + m_z * cos(\emptyset) * sin(\theta)}\right) \quad (2)$$

Here, Ψ_M is the magnetic heading, $\emptyset$ and θ are the roll and pitch angles obtained using raw data from the accelerometer and gyroscope by applying various filters.

2.4. Heading transformations

Several north directions are taken as a reference when calculating the heading angle. True North (TN), Magnetic North (MN), and Grid North (GN) are the different norths, each of one point in different directions (Figure 5). The magnetometer sensor is the main component of IMU, which allows heading estimation. This sensor gives a magnetic vector based on Earth's magnetic field. The heading determined by measuring the magnetic field is known as the magnetic heading since the Earth's geographic and magnetic poles do not coincide. Removing a magnetic declination from the magnetic heading is necessary to determine the true heading or the heading referred to the geographical North direction [39, 40]. GN refers to the direction of the grid in a plane coordinate system, typically aligned with the grid of a map projection. Converting the spherical surface of the globe into a flat surface results in the distinction between true north and grid north, also known as convergence. The projection and map location determine a given map's convergence [41].

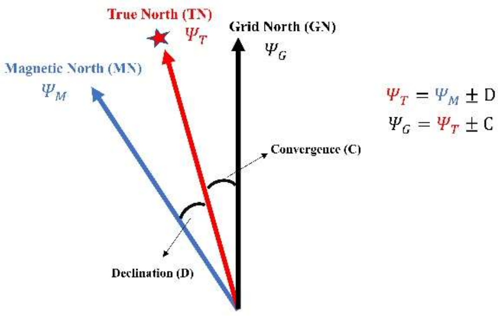

Figure 5. Magnetic, true, and grid north

Since the headings obtained with each sensor are in different systems, heading transformations were performed to compare them. The grid heading is taken as a reference for comparison.

2.5. Reference heading calculation

A line was determined for the study to compare the headings generated from sensors. In order to calculate the reference heading of this line, 15 points were determined on it and marked with spray, then three measurements of 30 epochs were made on each point, and 3D coordinates were obtained precisely by taking their averages (Figure 6). These point coordinates were obtained using Topcon Hiper V, which is based on the RTK/GNSS observation method, with an accuracy of 1-2 cm level. Then, the grid heading of the line was calculated using the coordinate data of 15 points. The reference heading of the line was calculated as 235.2594 degrees.

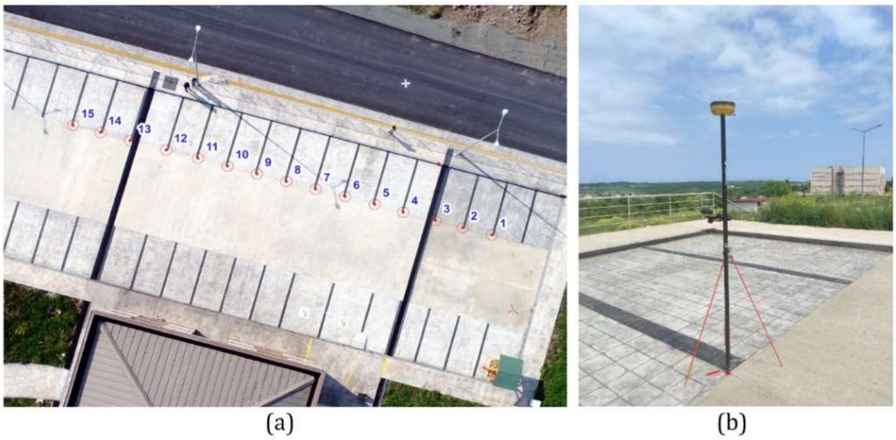

Figure 6. Test area (a) the line determined on which UGAV will track, (b) the measurement of the points on the line.

2.6. Field experiment: data collection of sensors

For the comparison of heading estimation capabilities of the sensors described in the previous sections, they were mounted on the UGAV. While collecting data with sensors, UGAV was driven along a line with starting point 1 and ending point 15. Before beginning the drive to get RTK fix solutions, convergence time was waited for the ambiguity resolution to be resolved. Sensor data collections were repeated seven times for seven different antenna conditions, and each measurement took approximately one minute. The manual calibration of IMUs was realised each time before starting the driving. The frequency of GNSS data collection was 1 Hz, whereas the IMU data were collected at 100 Hz.

3. Results and Discussion

After data collection in the field was completed, the heading values were estimated from the sensors' data using MATLAB software. For this purpose, geographical coordinates in GNGGA message type in NMEA format collected with GNSS were converted to the projection system (TM 3°). Then, the grid heading values were obtained using the coordinate values of each measurement according to Eq. 1. This makes approximately 60 measurements for GNSS data with a frequency of 1 Hz because each drive lasted approximately one minute. UTC has been converted to GPS Time of Week (ToW) to ensure time synchronization by using MATLAB software.

Xsens MTi 630 can generate true-heading, Euler angles, quaternions, and UTC in addition to the raw data, depending on the output options. In order to compare the heading of Xsens MTi 630 with the heading obtained from RTK/GNSS, time and heading transformations were made in MATLAB software. Thus, grid heading values of Xsens MTi 630 were obtained with GPS ToW. The data update frequency of Xsens MTi 630 was 100 Hz. This makes approximately 6000 measurements for one drive.

Magnetic heading values of Adafruit BNO055 were estimated using raw data of the sensors according to Eq. 2. Magnetic heading calculations from the raw data, transitions from magnetic heading to grid heading, and transitions from UTC to GPS ToW for time synchronisation were performed in MATLAB software. The data update frequency and number of measurements were the same with Xsens Mti 630.

The plots of the grid heading values and the reference grid heading value of each sensor in the same time interval for each antenna condition are shown in Figure 7. Antenna condition refers to the distances (baselines) between ANT1 and ANT2. In the 1st condition, the distance between the antennas is the farthest (210 cm), while in the 7th condition, the distance between the antennas is the closest (30 cm). The distance between antennas decreases by 30 cm from the 1st condition to the 7th condition.

For the first six cases where the baseline is long compared to condition seven, the heading accuracies of RTK/GNSS and Xsens MTi 630 are very close to each other and have almost the same characteristics. However, in condition seven, as the distance between antennas decreases to 30 cm, the heading accuracy of RTK/GNSS also decreases and is not like Xsens Mti 630. The heading accuracy of the Adafruit BNO055 is much noisier and more unstable than the other two sensors in all cases. Even though it seems to produce the most accurate results in case six, it is still below the other two sensors due to its noise. The sensors' respective comparisons in each case show that the Xsens MTi 630 provides similar accuracies for all conditions. Adafruit BNO055 appears to produce results with similar noise within a certain range. In the heading values obtained with RTK/GNSS, it is seen that the heading accuracy begins to decrease as the distance between antennas decreases. This decrease is not directly proportional to antenna distances. This decrease is not directly proportional to antenna distances as in the difference between conditions six and seven.

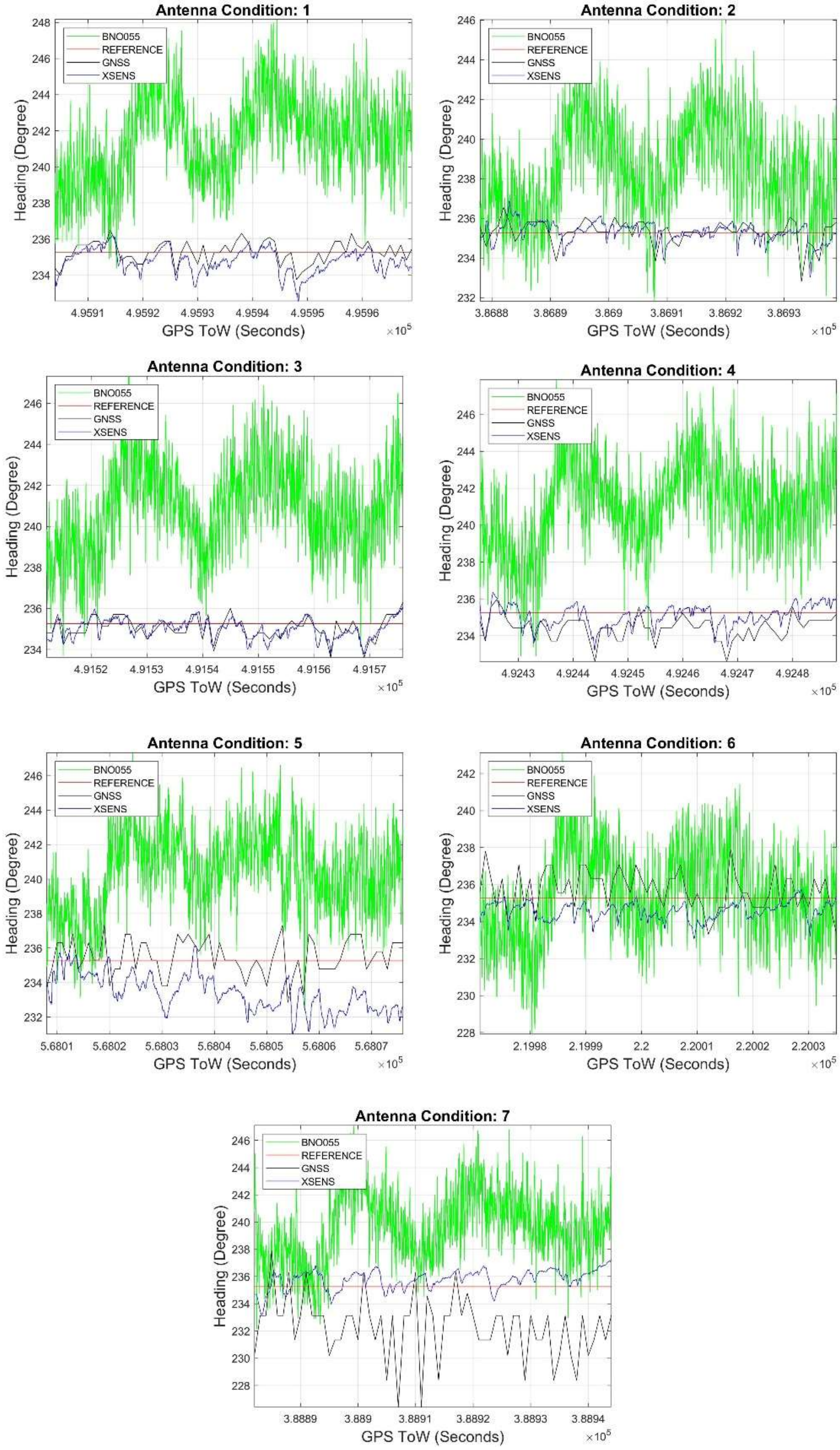

Figure 7. Heading plots of sensors and reference value

For a more quantitative comparison, the root mean square (RMS) error and mean values of the sensor headings in each case were calculated (Table 2). When the RMSs of GNSS-based headings are examined, the heading errors are relatively stable at first, with slight variations in RMS and mean values across the initial antenna conditions (one to three), where the antenna distance is 210 cm to 150 cm. As the antenna distance decreases (Conditions four through seven), both RMS and Mean heading errors tend to increase significantly. In Condition seven (30 cm distance), there is a sharp increase in heading error, with RMS rising from 0.8 to 3.7 degrees and the mean error increasing from 0.6 to 3.2 degrees. The significant increase in heading errors as the antenna distance decreases indicates that this sensor relies heavily on antenna separation for accurate heading determination. This matches the theoretical expectation that a larger baseline leads to better heading accuracy. The greater the baseline between the two antennas, the more accurate the measurement of the relative direction between the antennas as the relative position change between the two antennas becomes more noticeable, improving the accuracy of the heading calculation. Also, with a longer baseline, errors in individual position estimates of the antennas (due to noise or multipath) are less likely to affect the heading calculation. An extended baseline allows for better differentiation between the signals, making the heading determination less sensitive to minor errors.

Since the seventh condition does not accurately reflect the heading accuracy that can be achieved with RTK/GNSS, it is not included in calculating the average of the means of all conditions. When calculated this way, the average mean error of RTK/GNSS headings in all conditions except the seventh condition is 0.58 degrees.

The RMS values of the Xsens Mti 630 in each drive are generally close to each other, so it can be said that it has very high precision. The average mean error of Xsens Mti 630 headings in all conditions is 0.60 degrees. The Adafruit BNO055 sensor produced the worst results in terms of both accuracy and precision. The average mean error of BNO055, which produces quite noisy heading values, is 4.24 degrees.

Table 2. RMS and mean error values of sensors

	RMS (Degree)			Mean (Degree)		
Antenna Condition	SimpleRTK2B SBC	Xsens Mti 630	Adafruit BNO055	SimpleRTK2B SBC	Xsens Mti 630	Adafruit BNO055
1	0.6	0.8	6.8	0.5	0.6	6.3
2	0.6	0.5	3.9	0.4	0.4	3.3
3	0.6	0.5	6.0	0.5	0.4	5.6
4	0.8	0.9	4.5	0.6	0.7	4.0
5	0.8	0.8	4.7	0.6	0.6	4.1
6	1.1	0.8	2.4	0.9	0.7	2.0
7	3.7	0.9	5.0	3.2	0.8	4.4

Considering the sensor specifications, such as prices, advantages, and disadvantages (Table 1), the SimpleRTK2B is one of the most suitable sensors for high-accuracy applications in open-sky environments. In addition to providing heading performance and price equal to that of a tactical-grade IMU, it offers cm-level 3D position information. However, the distance between antennas affects the sensor's heading accuracy. The vehicle's dimensions used in the application must be considered to achieve maximum heading accuracy. The distance between the antennas should be above 60 cm for optimal results. In situations where the vehicle dimensions do not allow for optimal antenna spacing or indoor applications (e.g., greenhouses), the Xsens MTi 630 sensor should be preferred for high accuracy. This sensor can also generate position information indoors using a strap-down navigation approach. However, IMU sensors are sensitive to nearby metal objects. Calibration should be performed every time to minimise the effects of magnetic interference factors in the surroundings. For agricultural applications where high heading accuracy is not required, such as basic orientation tracking, the Adafruit BNO055 sensor, with its affordable price, may meet the user's needs. However, it should be noted that it does not provide UTC information. Additionally, the update rate in applications can also be an important component. The advantage of IMU sensors in this regard is noticeable. A high update rate allows for more precise tracking of fast-moving objects, making it especially beneficial in agricultural applications like automated machinery, crop monitoring, or robotic vehicles that require rapid response times. With a higher update rate, IMUs can provide more accurate and real-time orientation and movement data, leading to improved performance in dynamic environments. However, the trade-off is that high update rates can consume more power, which may be a consideration for battery-powered systems. Moreover, in applications where slower movement or less frequent updates are sufficient, the high update rate may lead to unnecessary data processing, potentially increasing computational load without providing significant benefits. Therefore, it is essential to balance the required accuracy with the system's power and computational capabilities.

In many studies, the performance of low-cost IMUs has not been tested independently. Instead, integrated solutions combining dual-antenna RTK/GNSS and low-cost IMUs have been developed to enhance robustness and accuracy. Furthermore, accuracy assessments in these studies are typically reported in terms of positional error [4, 15, 16, 25, 42, 43] rather than heading accuracy. Nevertheless, a comparative analysis has been conducted with a few studies that employ low-cost IMUs and RTK-GNSS sensors using similar accuracy evaluation criteria. Cui et al. [44] implemented a geometric-based path-tracking algorithm to guide an autonomous vehicle with a dual-antenna RTK and a navigation controller along a continuous U-shaped path. With an antenna baseline of 0.785 m, the system achieved a lateral position error within ±3 cm for 86.30% of the time and maintained a heading deviation within ±2 degrees for 90.61% of the time. Chen et al. [45] developed a coarse initial heading estimation method for the low-cost MEMS IMUs aided by the GNSS sensor. The initial heading is computed by comparing the two trajectories obtained with IMU-based and GNSS-based methods. The algorithm was tested on a car, a wheeled robot, and a tractor under various conditions. Results indicate that the initial heading was determined within 5 seconds with accuracies of 0.25, 0.6, and 1.6 degrees for the car, robot, and tractor, respectively. Galati et al. [46] developed a cost-efficient autonomous navigation system for agriculture by using a dual-antenna GPS and low-cost IMUs. The system utilises a Gaussian Sum Filter integrating multiple Extended Kalman Filters to address IMU bias and GPS signal loss. It achieved position and heading estimation, with average errors of 0.2 m and 0.2 degrees. Huang et al. [47] developed an integrated navigation system based on IMU and RTK-GNSS sensors to improve the positioning accuracy of autonomous agricultural vehicles. During operation on open roads, the system's position and heading errors are within 3 cm and 0.6 degrees, respectively. Pini et al. [48] evaluated the performance of the FANTASTIC GNSS receiver (simply FANTASTIC), which has dual antennas and integrated IMU. This sensor uses a loosely coupled GNSS/IMU integration to provide RTK-level position accuracy and GNSS-assisted attitude estimation. Three high-performance commercial GNSS receivers (Bmk1, Bmk2, and Bmk3) capable of delivering RTK measurements were considered benchmarks to compare FANTASTIC's performance. The performance of FANTASTIC was tested in four different environments: open-sky, kiwifruit orchard, vineyard, and greenhouse, alongside the benchmark GNSS receivers. Two reference systems, one GNSS-based and the other robotic total station-based, were used for evaluation. The heading error of FANTASTIC in open-field conditions was around 0.5 degrees. In the kiwifruit orchard, the heading error was 0.56 degrees with a 95% confidence level, while in the vineyard, it increased to 2.5 degrees with the same confidence level. Lastly, the heading error consistently remained above 1 degree in the greenhouse environment. Compared to previous studies, the results of this study are generally consistent with the high-precision findings reported in the literature.

4. Conclusion

In the agriculture industry, AVs and robots are useful tools for increasing productivity while lowering the need for human labour in various tasks. One of the most essential elements for AVs to successfully perform their tasks in the field is the ability to determine their heading correctly. GNSS and IMU are the most commonly used sensors to determine the heading of a vehicle. With the latest developments in sensor technology, systems with different accuracy and sensitivity have come along in every price range. This has initiated a quest for the most accurate results with the lowest possible price systems. Manufacturers of GNSS equipment have just begun to market small, RTK-capable, affordable receivers (less than $1,000). With the development of MEMS (Micro-Electro-Mechanical Systems) technology, IMU sensor sizes and costs have decreased.

The heading accuracies of low-cost RTK/GNSS, tactical grade, and low-cost MEMS IMUs were analysed in this context. Real driving tests were performed to study the heading performances of these sensors mounted on UGAV. Heading accuracies of GNSS RTK according to the distance between antennas and heading comparisons of GNSS RTK and other IMU sensors were evaluated. According to the RMS values in Table 2, RTK/GNSS produced the most accurate results when the antennas were furthest from each other. It shows that heading accuracy gradually deteriorates when the distance between antennas falls below 1.5 meters and deteriorates further when it falls below 60 cm. Therefore, a minimum antenna distance of 60 cm is recommended to obtain an accurate heading value with RTK/GNSS. RTK/GNSS and Xsens MTi 630 sensor generally gave similar results except for the 7th condition. If the distance between antennas is sufficient, it can be seen that RTK/GNSS can achieve the accuracy of a tactical-grade IMU.

The low-cost Adafruit BNO055 IMU sensor produced the noisiest results. It has an average mean error that may be sufficient for applications that do not require very precise heading information. For example, it can track the general movement direction of tractors or agricultural vehicles in large fields or where precise row planting is not required. However, for precision agriculture applications such as auto-steering, precise spraying systems and row planting, this accuracy may not be acceptable. In such cases, RTK-GNSS or high-accuracy IMUs should be preferred.

Acknowledgment

This work was supported by the Ondokuz Mayis University under Grant PYO.MUH.1908.22.078.

Conflict of Interest Statement

The authors declare that there is no conflict of interest

References

[1] D. T. Fasiolo, L. Scalera, E. Maset, and A. Gasparetto, "Towards autonomous mapping in agriculture: A review of supportive technologies for ground robotics," *Rob Auton Syst,* vol. 169, Nov. 2023. doi: 10.1016/j.robot.2023.104514

[2] K. R. Aravind, P. Raja, and M. Pérez-Ruiz, "Task-based agricultural mobile robots in arable farming: A review," *Spanish Journal of Agricultural Research*, vol. 15, no. 1, 2017. doi: 10.5424/sjar/2017151-9573

[3] A. Ghobadpour, G. Monsalve, A. Cardenas, and H. Mousazadeh, "Off-Road Electric Vehicles and Autonomous Robots in Agricultural Sector: Trends, Challenges, and Opportunities," *Vehicles*, vol. 4, no. 3, pp. 843-864, 2022. doi: 10.3390/vehicles4030047

[4] M. Nørremark, H. W. Griepentrog, J. Nielsen, and H. T. Søgaard, "The development and assessment of the accuracy of an autonomous GPS-based system for intra-row mechanical weed control in row crops," *Biosystems Engineering*, vol. 101, no. 4, pp. 396–410, 2008. doi: 10.1016/j.biosystemseng.2008.09.007

[5] A. T. Meshram, A. V. Vanalkar, K. B. Kalambe, and A. M. Badar, "Pesticide spraying robot for precision agriculture: A categorical literature review and future trends," *Journal of Field Robotics*, vol. 39, no. 2, pp. 153–171, 2022. doi: 10.1002/rob.22043

[6] W. Ji, D. Zhao, F. Cheng, B. Xu, Y. Zhang, and J. Wang, "Automatic recognition vision system guided for apple harvesting robot," *Computers and Electrical Engineering*, vol. 38, no. 5, pp. 1186–1195, 2012. doi: 10.1016/j.compeleceng.2011.11.005

[7] Y. Zhao, L. Gong, C. Liu, and Y. Huang, "Dual-arm Robot Design and Testing for Harvesting Tomato in Greenhouse," *IFAC-PapersOnLine,* vol. 49, no. 16, pp. 161–165, 2016. doi: 10.1016/j.ifacol.2016.10.030

[8] H. Zhou, X. Wang, W. Au, H. Kang, and C. Chen, "Intelligent robots for fruit harvesting: recent developments and future challenges," *Precision Agriculture*, vol. 23, pp. 1856-1907, 2022. doi: 10.1007/s11119-022-09913-3

[9] P. Gonzalez-de-Santos, A. Ribeiro, C. Fernandez-Quintanilla, et al., "Fleets of robots for environmentally-safe pest control in agriculture," *Precision Agriculture*, vol. 18, no. 4, pp. 574–614, 2017. doi: 10.1007/s11119-016-9476-3

[10] T. L. Oluwabunmi, O. Adenugba, I. A. Ayoade, J. Azeta, and C. A. Bolu, "Development of an Autonomous Vehicle for Smart Irrigation," in *2022 5th Information Technology for Education and Development (ITED),* Abuja, Nigeria, November 1-3, 2022, IEEE, pp. 1-7. doi: 10.1109/ITED56637.2022.10051388

[11] A. Bechar and C. Vigneault, "Agricultural robots for field operations. Part 2: Operations and systems," *Biosystems Engineering, vol. 153*, pp. 110–128, 2017. doi: 10.1016/j.biosystemseng.2016.11.004

[12] Y. Bai, B. Zhang, N. Xu, J. Zhou, J. Shi, and Z. Diao, "Vision-based navigation and guidance for agricultural autonomous vehicles and robots: A review," *Computers and Electronics in Agriculture*, vol. 205, no. 107584, 2023. doi: 10.1016/j.compag.2022.107584

[13] T. Bakker, K. van Asselt, J. Bontsema, J. Müller, and G. van Straten, "Autonomous navigation using a robot platform in a sugar beet field," *Biosystems Engineering*, vol. 109, no. 4, pp. 357–368, 2011. doi: 10.1016/j.biosystemseng.2011.05.001

[14] X. Han, H. J. Kim, C. W. Jeon, H. C. Moon, J. H. Kim, and S. Y. Yi, "Application of a 3D tractor-driving simulator for slip estimation-based path-tracking control of auto-guided tillage operation," *Biosystems Engineering*, vol. 178, pp. 70–85, 2019. doi: 10.1016/j.biosystemseng.2018.11.003

[15] S. Alonso-Garcia, J. Gomez-Gil, and J. I. Arribas, "Evaluation of the use of low-cost GPS receivers in the autonomous guidance of agricultural tractors," *Spanish Journal of Agricultural Research*, vol. 9, no. 2, pp. 378–388, 2011. [Online]. Available: www.inia.es/sjar

[16] J. H. Han, C. H. Park, Y. J. Park, and J. H. Kwon, "Preliminary results of the development of a single-frequency GNSS RTK-based autonomous driving system for a speed sprayer," *Journal of Sensors*, vol. 2019, no. 1, 2019. doi: 10.1155/2019/4687819

[17] A. Leanza, R. Galati, A. Ugenti, E. Cavallo, and G. Reina, "Where am I heading? A robust approach for orientation estimation of autonomous agricultural robots," *Computers and Electronics in Agriculture*, vol. 210, Jul. 2023. doi: 10.1016/j.compag.2023.107888

[18] A. Mizushima, K. Ishii, N. Noguchi, Y. Matsuo, and R. Lu, "Development of a low-cost attitude sensor for agricultural vehicles," *Computers and Electronics in Agriculture*, vol. 76, no. 2, pp. 198–204, May 2011. doi: 10.1016/j.compag.2011.01.017

[19] D. Jiang, L. Yang, D. Li, F. Gao, L. Tian, and L. Li, "Development of a 3D ego-motion estimation system for an autonomous agricultural vehicle," *Biosystems Engineering*, vol. 121, pp. 150–159, 2014. doi: 10.1016/j.biosystemseng.2014.02.016

[20] A. Roshanianfard, N. Noguchi, H. Okamoto, and K. Ishii, "A review of autonomous agricultural vehicles (The experience of Hokkaido University)," *Journal of Terramechanics*, vol. 91, pp. 155-183, October 2020. doi: 10.1016/j.jterra.2020.06.006

[21] S. Sasani, J. Asgari, and A. R. Amiri-Simkooei, "Improving MEMS-IMU/GPS integrated systems for land vehicle navigation applications," *GPS Solutions*, vol. 20, no. 1, pp. 89–100, Jan. 2016. doi: 10.1007/s10291-015-0471-3

[22] Y. Li, M. Efatmaneshnik, and A. G. Dempster, "Attitude determination by integration of MEMS inertial sensors and GPS for autonomous agriculture applications," *GPS Solutions*, vol. 16, no. 1, pp. 41–52, Jan. 2012. doi: 10.1007/s10291-011-0207-y

[23] L. Cong, E. Li, H. Qin, K. V. Ling, and R. Xue, "A performance improvement method for low-cost land vehicle GPS/MEMS-INS attitude determination," *Sensors*, vol. 15, no. 3, pp. 5722–5746, Mar. 2015. doi: 10.3390/s150305722

[24] J. Si, Y. Niu, J. Lu, and H. Zhang, "High-Precision Estimation of Steering Angle of Agricultural Tractors Using GPS and Low-Accuracy MEMS," *IEEE Transactions on Vehicular Technology*, vol. 68, no. 12, pp. 11738–11745, Dec. 2019. doi: 10.1109/TVT.2019.2949298

[25] J. H. Han, C. H. Park, Y. Y. Jang, J. D. Gu, and C. Y. Kim, "Performance evaluation of an autonomously driven agricultural vehicle in an orchard environment," *Sensors*, vol. 22, no. 1, Jan. 2022. doi: 10.3390/s22010114

[26] J. Jackson, R. Saborio, S. A. Ghazanfar, D. Gebre-Egziabher, and B. Davis, "Evaluation of Low-Cost, Centimeter-Level Accuracy OEM GNSS Receivers," *the University Digital Conservancy*, 2018. Available: https://hdl.handle.net/11299/197453.2018

[27] M. Farkas, S. Rózsa, and B. Vanek, "Multi-sensor Attitude Estimation using Quaternion Constrained GNSS Ambiguity Resolution and Dynamics-Based Observation Synchronization," *Acta Geodaetica et Geophysica*, vol. 59, pp. 51-71, Mar. 2024. doi: 10.1007/s40328-024-00441-2

[28] N. Nadarajah, P. J. G. Teunissen, and N. Raziq, "Instantaneous GPS-galileo attitude determination: Single-frequency performance in satellite-deprived environments," *IEEE Transactions on Vehicular Technology*, vol. 62, no. 7, pp. 2963–2976, 2013. doi: 10.1109/TVT.2013.2256153

[29] F. Zhu, Z. Hu, W. Liu, and X. Zhang, "Dual-Antenna GNSS Integrated with MEMS for Reliable and Continuous Attitude Determination in Challenged Environments," *IEEE Sensors Journal*, vol. 19, no. 9, pp. 3449–3461, May 2019. doi: 10.1109/JSEN.2019.2891783

[30] J. Y. Huang, Z. Y. Huang, and K. H. Chen, "Combining Low-Cost Inertial Measurement Unit (IMU) and Deep Learning Algorithm for Predicting Vehicle Attitude," in *IEEE Conference on Dependable and Secure Computing*, Taipei, Taiwan, October 7-10, 2017, IEEE, pp. 237–239. doi: 10.1109/DESEC.2017.8073847

[31] A. H. Işık and Ö. Çetin, "Multifunctional and Low Cost Autonomous Mobile Robot," *Gazi Journal of Engineering Sciences*, vol. 6, no. 2, pp. 105–110, Aug. 2020. doi: 10.30855/gmbd.2020.02.02

[32] ArduSimple, "SimpleRTK2B SBC - Development Kit." Accessed: May 28, 2024. [Online]. Available: https://www.ardusimple.com/product/simplertk2b-sbc-development-kit/

[33] S. Ji, R. Du, W. Chen, Z. Wang, K. He, and Z. Nie, "Partial GNSS ambiguity resolution in coordinate domain," *Survey Review*, vol. 51, no. 369, pp. 525–532, Nov. 2019. doi: 10.1080/00396265.2018.1490870

[34] u-blox, "ZED-F9P Moving base applications Application note: ZED-F9P-MovingBase_AppNote_UBX-19009093," 2023. [Online]. Available: www.u-blox.com

[35] J. Keong and G. Lachapelle, "Heading and Pitch Determination Using GPS/GLONASS," *GPS Solutions*, vol. 3, pp. 26-36, 2000. Available: https://doi.org/10.1007/PL00012800

[36] Xsens, "Xsens MTi 630." Accessed: May 28, 2024. [Online]. Available: https://www.movella.com/products/sensor-modules/xsens-mti-630-ahrs

[37] Adafruit, "BNO055 Intelligent 9-axis absolute orientation sensor," 2016. [Online]. Available: https://www.bosch-sensortec.com/products/smart-sensor-systems/bno055/

[38] X. Cui, Y. Li, Q. Wang, M. Karaim, and A. Noureldin, "Vehicle heading estimation of INS/magnetometer integrated system based on constant hard iron interference calibration," Measurement and Control, vol. 54, no. 7–8, pp. 1208–1218, Sep. 2021, doi: 10.1177/00202940211021876

[39] P. Kaniewski and J. Kazubek, "Integrated System for Heading Determination," *Acta Physica Polonica A*, vol. 116, no. 3, pp. 325-330, 2009.

[40] B. Li, T. Gallagher, A. G. Dempster, and C. Rizos, "How feasible is the use of magnetic field alone for indoor positioning?" in *2012 International Conference on Indoor Positioning and Indoor Navigation,* Sydney, NSW, Australia, November 13-15, 2012, IEEE, pp. 1-9. doi: 10.1109/IPIN.2012.6418880

[41] USGS, "What do the different north arrows on a USGS topographic map mean?" Accessed: May 29, 2024. [Online]. Available: https://www.usgs.gov/faqs/what-do-different-north-arrows-usgs-topographic-map-mean

[42] A. Stoll and H. D. Kutzbach, "Guidance of a Forage Harvester with GPS," *Precision Agriculture*, vol. 2, pp. 281–291, 2000.

[43] J. Carballido, M. Perez-Ruiz, L. Emmi, and J. Agüera, "Comparison of Positional Accuracy between RTK and RTX GNSS based on The Autonomous Agricultural Vehicles under Field Conditions," *Applied Engineering in Agriculture*, vol. 30, no. 3, pp. 361–366, 2014. doi: 10.13031/aea.30.10342

[44] B. Cui, J. Zhang, X. Wei, X. Cui, Z. Sun, Y. Zhao, and Y. Liu, "Improved Information Fusion for Agricultural Machinery Navigation Based on Context-Constrained Kalman Filter and Dual-Antenna RTK," *Actuators*, vol. 13, no. 5, 2024. doi: 10.3390/act13050160

[45] Q, Chen, H. Lin, J. Kuang, Y. Luo, and X. Niu, "Rapid Initial Heading Alignment for MEMS Land Vehicular GNSS/INS Navigation System," *IEEE Sensors Journal*, vol. 23, no. 7, pp. 7656–7666, 2023. doi: 10.1109/JSEN.2023.3247587

[46] R. Galati, G. Mantriota, and G. Reina, "RoboNav: An Affordable Yet Highly Accurate Navigation System for Autonomous Agricultural Robots," *Robotics*, vol. 11, no. 5, 2022. doi: 10.3390/robotics11050099

[47] Y. Huang, J. Fu, S. Xu, T. Han, and Y. Liu, "Research on Integrated Navigation System of Agricultural Machinery Based on RTK-BDS/INS," *Agriculture*, vol. 12, no. 8, 2022. doi: 10.3390/agriculture12081169

[48] M. Pini, G. Marucco, G. Falco, M. Nicola, and W. De Wilde, "Experimental Testbed and Methodology for the Assessment of RTK GNSS Receivers Used in Precision Agriculture," *IEEE Access*, vol. 8, pp. 14690–14703, 2020. doi: 10.1109/ACCESS.2020.2965741